Molecular Cell
Article

Roles of R2D2, a Cytoplasmic D2 Body Component, in the Endogenous siRNA Pathway in *Drosophila*

Kazumichi M. Nishida,[1,4] Keita Miyoshi,[1,4,5] Akiyo Ogino,[1,2,4] Tomohiro Miyoshi,[1,6] Haruhiko Siomi,[1] and Mikiko C. Siomi[1,3,7,*]

[1]Department of Molecular Biology, Keio University School of Medicine, Tokyo 160-8582, Japan
[2]Graduate School of Environment and Information Science, Yokohama National University, Yokohama 240-8501, Japan
[3]JST, CREST, Saitama 332-0012, Japan
[4]These authors contributed equally to this work
[5]Present address: School of Medicine and Dentistry, University of Rochester, Rochester, NY 14642, USA
[6]Present address: Center for Transdisciplinary Research, Niigata University, Niigata 950-2181, Japan
[7]Present address: Graduate School of Science, The University of Tokyo, Tokyo 113-0032, Japan
*Correspondence: siomim@biochem.s.u-tokyo.ac.jp
http://dx.doi.org/10.1016/j.molcel.2012.12.024

SUMMARY

Endogenous small interfering RNAs (endo-siRNAs) in *Drosophila* are processed by Dicer-2 (Dcr-2) and loaded onto Ago2 by the Dcr-2/R2D2 heterodimer. In *r2d2* mutants, the level of endo-siRNAs is unchanged, but endo-siRNAs are misloaded onto Ago1. However, the mechanism underlying the control of endo-siRNA sorting by R2D2 remains unknown. Here, we show that R2D2 controls endo-siRNA sorting by localizing Dcr-2, and presumably endo-siRNA duplexes, to cytoplasmic foci, D2 bodies. Ago2, but not Ago1, localized to D2 bodies. dsRNA-binding-deficient mutant, but not wild-type, R2D2 failed to localize D2 bodies and caused endo-siRNA misdirection to Ago1 in R2D2-depleted cells. However, R2D2 was dispensable for sorting miRNAs and exogenous siRNAs onto Ago1 and Ago2, respectively, in vivo. Endo- and exo-siRNA guide selection also occurred R2D2 independently. The functions of R2D2 are required to avoid endo-siRNA misdirection to Ago1, because Ago1 is capable of loading incompletely complementary miRNA duplexes and endo-siRNA duplexes.

INTRODUCTION

In RNA silencing, a small noncoding RNA associates with an Argonaute protein, the effector protein in the RNA silencing machinery, to form the RNA-induced silencing complex (RISC) and guides the RISC to their target RNAs to regulate cellular gene networks and physiological processes in living organisms (Siomi and Siomi, 2009). Animals express three types of endogenous small RNAs: microRNAs (miRNAs), PIWI-interacting RNAs (piRNAs), and endogenous small interfering RNAs (endo-siRNAs) (Ghildiyal and Zamore, 2009; Kim et al., 2009; Siomi et al., 2011). These small RNAs can be classified based on their origins, processing factors, and Argonaute binding partners (Ghildiyal and Zamore, 2009; Kim et al., 2009; Czech and Hannon, 2011).

miRNAs are processed from their primary precursors by two RNase III enzymes, Drosha and Dicer, in tandem, in the nucleus and the cytoplasm, respectively (Denli et al., 2004; Gregory et al., 2004; Lee et al., 2003). *Drosophila* possesses two *Dicer* genes, *Dicer-1* (*Dcr-1*) and *Dicer-2* (*Dcr-2*), and miRNA processing requires *Dcr-1*, but not *Dcr-2* (Lee et al., 2004). Upon maturation following Dcr-1 processing, miRNAs in *Drosophila* are principally associated with Argonaute 1 (Ago1) to form the miRISC (Miyoshi et al., 2009; Okamura et al., 2004).

Like piRNAs, endo-siRNAs originate from intergenic DNA elements. However, in contrast to piRNA biogenesis, which occurs *Dicer* independently, endo-siRNA biogenesis in *Drosophila* requires *Dcr-2* (Vagin et al., 2006; Czech et al., 2008; Ghildiyal et al., 2008; Kawamura et al., 2008; Okamura et al., 2008). Dcr-2 was originally identified as an enzyme responsible for processing exogenous siRNAs (exo-siRNAs) from long double-stranded RNA (dsRNA) precursors such as viral genomes (Bernstein et al., 2001; Lee et al., 2004; Liu et al., 2003). Therefore, it is most likely that the endo-siRNA precursors are double-stranded RNAs. After maturation, endo-siRNAs are loaded onto Ago2 to form the endo-siRISC, which silences transposons and some protein-coding genes (Czech et al., 2008; Ghildiyal et al., 2008; Kawamura et al., 2008; Okamura et al., 2008).

RNase III enzymes associate with dsRNA-binding proteins (dsRBPs) during small RNA biogenesis. *Drosophila* Dcr-1 associates with Loquacious (Loqs; also known as R3D1) (Förstemann et al., 2005; Jiang et al., 2005; Saito et al., 2005). The *Loqs* gene gives rise to four isoforms, Loqs-PA, Loqs-PB, Loqs-PC, and Loqs-PD (Hartig et al., 2009). The longest isoform, Loqs-PB, facilitates miRNA processing by Dcr-1 (Hartig et al., 2009; Marques et al., 2010; Miyoshi et al., 2010; Zhou et al., 2009). Mutations in Loqs-PD cause a severe reduction in the accumulation of endo-siRNAs in vivo, but the level of expression of Dcr-2 is unchanged by Loqs-PD depletion, suggesting a direct role of Loqs-PD in endo-siRNA processing (Hartig et al., 2009; Marques et al., 2010; Miyoshi et al., 2010; Zhou et al., 2009).

Another dsRBP, R2D2, associates with Dcr-2 but is dispensable for exo-siRNA excision from precursors in vitro (Liu et al.,

2003). However, the Dcr-2/R2D2 heterodimer constituting the RISC-loading complex (RLC) enhances exo-siRNA loading onto Ago2 (Liu et al., 2003, 2006; Pham et al., 2004; Tomari et al., 2004, 2007). In the loading phase, the RLC senses the thermodynamic asymmetry of both ends of exo-siRNA duplexes (Khvorova et al., 2003; Liu et al., 2003; Schwarz et al., 2003; Tomari et al., 2004, 2007). The exo-siRNA with the less stable 5′ end is selected and preferentially incorporated into the RISC. The other strand is eventually degraded in the cellular environment.

R2D2 is unnecessary for endo-siRNA accumulation (Czech et al., 2008; Ghildiyal et al., 2008; Marques et al., 2010; Okamura et al., 2008; Zhou et al., 2009). However, endo-siRNAs, which are 2′-*O*-methylated at the 3′ end, became sensitive to β-elimination in *r2d2* mutants (Ghildiyal et al., 2008). β-elimination sensitivity is the hallmark of miRNAs associated with Ago1 in *Drosophila*, suggesting that endo-siRNAs would be misloaded onto Ago1 without R2D2 expression. Indeed, endo-siRNAs were misdirected to Ago1 in cells lacking R2D2 (Ameres et al., 2011; Marques et al., 2010; Okamura et al., 2011). Loqs and R2D2 act sequentially in exo-/endo-siRNA processing and loading, respectively (Marques et al., 2010). These observations support the idea that R2D2, which is dispensable for endo-siRNA processing, plays a crucial role(s) in endo-siRNA sorting and loading. However, the underlying mechanism remains unknown.

In this study, we found that endogenous Dcr-2 and R2D2 localize to cytoplasmic foci in *Drosophila* cells. Chemicals affecting cytoplasmic structures, processing bodies (P bodies) and stress granules (SGs), had little or no effects on the Dcr-2-positive foci in Schneider 2 (S2) cells; thus, the bodies were designated D2 bodies. Both Dcr-2 and R2D2 are necessary for D2 body formation, but in distinct ways: Dcr-2 stabilizes R2D2, whereas R2D2 localizes Dcr-2 to D2 bodies. Overexpression of R2D2 restores dotty structures similar to D2 bodies in Dcr-2-depleted cells; thus, R2D2 is likely critical for D2 body formation. endo-siRNAs, but not exo-siRNAs, were misdirected to Ago1 in R2D2-depleted S2 cells, where the guide strands of both exo- and endo-siRNA duplexes were selectively loaded onto Ago2; thus, R2D2 is dispensable for guide strand selection and Ago2-specific loading of exo-siRNAs. Wild-type (WT) R2D2, but not dsRNA-binding-defective mutant R2D2, rescued the defects in D2 body formation and endo-siRNA sorting onto Ago2 caused by loss of R2D2. These results suggest that R2D2 ensures endo-siRNA sorting by localizing Dcr-2, and presumably endo-siRNA duplexes, to D2 bodies, where Ago2, but not Ago1, is localized. R2D2 functions are required to avoid endo-siRNA misdirection to Ago1 because Ago1 is capable for loading incompletely complementary miRNA duplexes and endo-siRNA duplexes.

RESULTS

Dcr-2 Localizes to Cytoplasmic D2 Bodies

Immunostaining of S2 cells with anti-Dcr-2 antibodies (Miyoshi et al., 2010) revealed that endogenous Dcr-2 accumulates into cytoplasmic foci (Figure 1A). To determine if the dotty signals reflect the Dcr-2 localization per se, we immunostained Dcr-2-depleted S2 cells. While a control siRNA against EGFP did not affect the Dcr-2-positive foci (Figure 1B; EGFP RNAi), depletion of Dcr-2 caused disappearance of these bodies (Figure 1B; Dcr-2 RNAi), confirming that Dcr-2 accumulates in cytoplasmic bodies.

The Dcr-2 punctate signals looked similar to those of well-characterized cytoplasmic structures, P bodies and SGs (Eulalio et al., 2007a). To examine the relationship between the Dcr-2-positive foci and P bodies, S2 cells were double stained with anti-Dcr-2 and anti-Dcp1 antibodies (Miyoshi et al., 2009). Dcp1 is a component of an mRNA-decapping complex and a marker of P bodies (Eulalio et al., 2007a). The Dcr-2-positive foci partially overlapped with P bodies (Figure 1C). Treatment of S2 cells with two chemicals, cycloheximide that stalls ribosomes on mRNAs and puromycin that disassembles ribosomes from translating mRNAs, caused fragmentation and enlargement of P bodies, respectively (Figure 1C), as has been reported previously (Eulalio et al., 2007a, 2007b). Two other components of P bodies, Trailer hitch (Tral) and Me31B (Barbee et al., 2006), behaved similarly to Dcp1 (see Figure S1A online). In contrast, Dcr-2-positive structures were not affected by the chemical treatments (Figure 1C and Figure S1A). Depletion of Dcr-2 did not affect Dcp1 localization in S2 cells (Figure S1B). Thus, the Dcr-2-positive bodies are distinct from P bodies.

Cellular stresses, such as increased temperature, a highly oxidative environment, and UV irradiation, cause bulk mRNAs to be accumulated into SGs and inhibit their translation (Farny et al., 2009; Kedersha et al., 2005). SGs are formed in very close proximity to P bodies (Kedersha et al., 2005; Farny et al., 2009), raising the possibility that the Dcr-2-positive foci might correspond to SGs. To examine this possibility, S2 cells were immunostained with anti-Dcr-2 and anti-dFMR1 antibodies. dFMR1 is a KH-domain-containing RNA-binding protein encoded by *dFmr1*, a fly ortholog of the *fragile X mental retardation gene 1* (*Fmr1*) in mammals (Wan et al., 2000). dFMR1 strongly accumulates in SGs under stress conditions and thus can be used as a SG marker (Farny et al., 2009). Under nonstress conditions, weak dFMR1 signals overlapped with Dcr-2 signals (Figure 1D). Arsenite treatment leading to an increase in the number of SGs and their enlargement (Farny et al., 2009) drastically changed the dFMR1 staining patterns, but not the Dcr-2 signals (Figure 1D), indicating that the Dcr-2-positive foci are not SGs. The punctuate Dcr-2 signals did not overlap with those for dGM130, a protein that is strongly attached to Golgi membranes (Figure 1E) (Kondylis et al., 2001; Yano et al., 2005). We designate them D2 bodies.

R2D2, a Component of D2 Bodies, Is Necessary for D2 Body Formation

R2D2 tightly associates with Dcr-2 (Liu et al., 2003; Miyoshi et al., 2010); thus, we postulated that R2D2 might also localize to D2 bodies. Immunofluorescence using anti-R2D2 (Figure S2A) and anti-Dcr-2 antibodies revealed that R2D2 colocalizes with Dcr-2 to D2 bodies (Figure 2A and Figure S2B). Foci similar to D2 bodies were observed with both antibodies in ovarian follicle cells of a fly line overexpressing Dcr-2, $dcr\text{-}2^{25708}$ (Figure S2B). Nurse cells and oocytes showed no dotty structures corresponding to D2 bodies (Figure S2C). It remains unknown

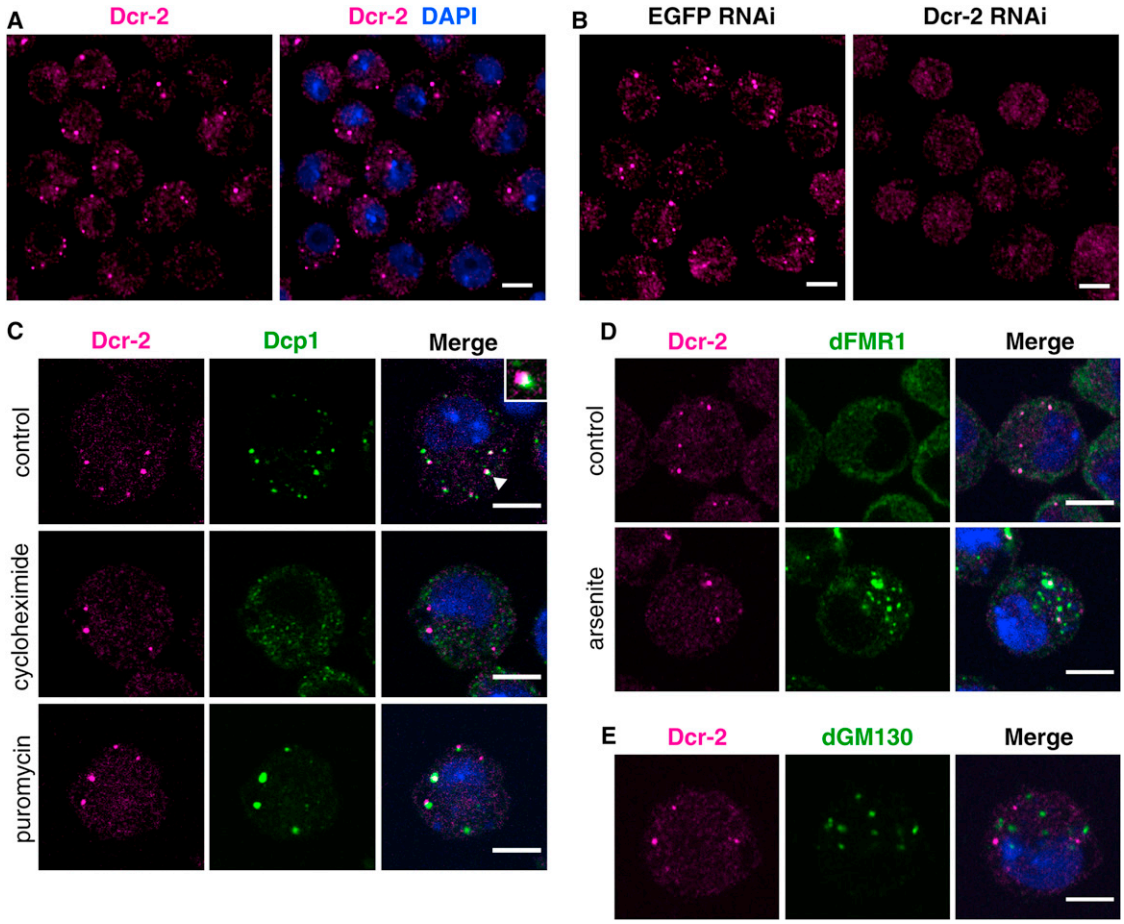

Figure 1. Dcr-2 Localizes to Cytoplasmic Granules, D2 Bodies, in *Drosophila* S2 Cells

(A) S2 cells immunostained with an anti-Dcr-2 antibody show strong foci exclusively located in the cytoplasm. Nuclei are stained with DAPI (blue). Scale bars, 5 μm.

(B) The punctate signals in (A) disappeared when Dcr-2 was depleted by RNAi (Dcr-2 RNAi). EGFP dsRNA, used as a control, had little or no effect on Dcr-2 signals (EGFP RNAi). Scale bars, 5 μm.

(C) Cycloheximide and puromycin treatments cause changes in the shape and size of P bodies (Dcp1,) but not those of the Dcr-2-positive foci. The inset (top right), an enlarged image of the structure indicated by a white arrowhead, clearly shows that the signals for Dcr-2 and Dcp1 partially overlap. Nuclei are stained with DAPI (blue). Scale bars, 5 μm.

(D) Arsenite treatment enlarges SGs (dFMR1) but not Dcr-2-positive foci. Nuclei are stained with DAPI (blue). Scale bars, 5 μm.

(E) The Dcr-2-positive foci do not overlap with Golgi structures (dGM130). Nuclei are stained with DAPI (blue). Scale bars, 5 μm. See also Figure S1.

if nurse cells and oocytes express endo-siRNAs. Thus, R2D2 colocalization with Dcr-2 is not a specific event in cultured S2 cells.

To examine the mutual dependency of Dcr-2 and R2D2 in D2 body localization, both proteins were respectively depleted from S2 cells by RNAi. R2D2 depletion caused disappearance of D2 bodies (Figure 2A). The expression level of Dcr-2 was little changed by R2D2 depletion (Figure 2A). This is consistent with the previous finding that the level of Dcr-2 is maintained in *r2d2* null mutant flies (Liu et al., 2006). These results suggest that Dcr-2 localization to D2 bodies depends on the presence of R2D2 in *Drosophila* cells.

Depletion of Dcr-2 also induced loss of D2 bodies (Figures 1B and 2B and Figure S2D). Western blotting revealed that Dcr-2 RNAi greatly reduced the levels of not only Dcr-2 but also R2D2 (Figure 2B). This also confirmed the previous finding that Dcr-2 stabilizes R2D2 in vivo (Liu et al., 2006). The R2D2 dotty signals were hardly detected in Dcr-2-depleted cells, as expected (Figure 2B and Figure S2D). Thus, D2 body formation requires both Dcr-2 and R2D2, but in distinct ways; Dcr-2 is required for stabilizing R2D2, while R2D2 is required for localizing Dcr-2 to D2 bodies.

We then overexpressed Flag-tagged R2D2 in Dcr-2-depleted S2 cells. Western blotting confirmed that the expression of Flag-R2D2 was maintained in Dcr-2-depleted cells, in which Dcr-2 silencing was still effective (Figure 2C). Flag-R2D2 accumulated in cytoplasmic foci without Dcr-2 expression, demonstrating that R2D2 has the ability to form the dotty structures even in the absence of Dcr-2 (Figure 2C and Figure S2E). Thus, R2D2 might be a core component of D2 bodies.

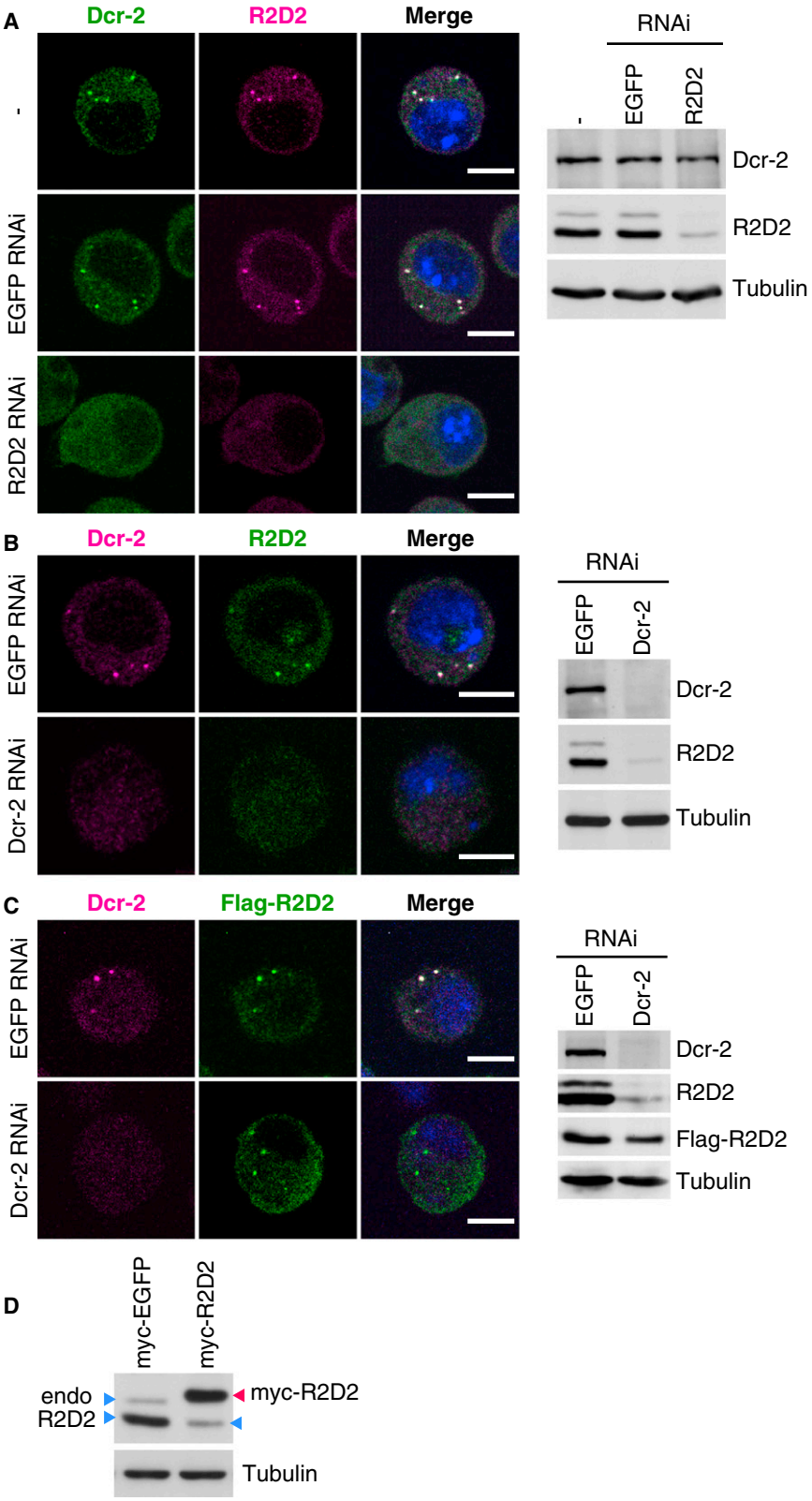

Figure 2. Formation of D2 Bodies Requires Both R2D2 and Dcr-2

(A) (Left) RNAi for R2D2, but not EGFP, causes disappearance of D2 bodies in S2 cells. Nuclei are stained with DAPI (blue). Scale bars, 5 μm. (Right) Western blotting shows that R2D2 RNAi downregulates R2D2 greatly but does not alter the expression level of Dcr-2. Tubulin was detected as an internal control.

(B) (Left) RNAi for Dcr-2, but not EGFP, causes disappearance of D2 bodies in S2 cells. Scale bars, 5 μm. (Right) Dcr-2 RNAi downregulates not only Dcr-2 but also R2D2. Dcr-2 is necessary for stabilizing R2D2.

(C) (Left) Flag-R2D2 overexpressed in Dcr-2-depleted cells accumulates in cytoplasmic foci similar to D2 bodies. Scale bars, 5 μm. (Right) Western blotting shows that Flag-R2D2 is expressed in S2 cells where Dcr-2 is still downregulated.

(D) Western blotting of total S2 lysates using an anti-R2D2 antibody shows that expression of myc-R2D2 (red arrowhead), but not that of myc-EGFP, causes a severe decrease in the level of endogenous R2D2 (blue arrowheads). Tubulin was detected as an internal loading control. See also Figure S2.

In the course of our experiments, we noticed that overexpression of myc-tagged R2D2 in S2 cells resulted in a severe reduction in the level of endogenous R2D2 (Figure 2D). The number of D2 bodies looked the same before and after myc-R2D2 and Flag-R2D2 overexpression (Figure 2C and Figure S2F). The simplest scenario to explain these observations is that myc-R2D2 substituted for endogenous R2D2 in D2 bodies and that endogenous R2D2 that had been displaced from D2 bodies was degraded in the cytosol via an unknown mechanism. These results suggest that D2 bodies are likely composed of Dcr-2 and R2D2 in a stoichiometric manner. Quantification of the Dcr-2 and R2D2 signals in S2 cells revealed that Dcr-2 and R2D2 in D2 bodies make up ~8.6% and ~5.5%, respectively, of the total amounts of Dcr-2 and R2D2 per cell, respectively (Figure S2G). Loss of Dcr-2 destabilizes R2D2 (Figure 2B). Thus, R2D2 may interact with Dcr-2 even outside of D2 bodies.

Depletion of Dcr-1, Ago2, and all Loqs isoforms did not affect appearance of D2 bodies (Figure S2H), indicating that these factors, including Loqs-PD, are dispensable for D2 body formation. myc-Loqs-PD expressed via a transgene did not specifically localize to D2 bodies (Miyoshi et al., 2010). Thus, Loqs-PD may not be a constituent of D2 bodies, unlike R2D2.

Association with R2D2 Is Necessary for Dcr-2 to Localize to D2 Bodies

To determine which region of Dcr-2 is required for its localization to D2 bodies, Dcr-2 was divided in half to yield two deletion mutants, N950 (residues 1–950) and C951 (residues 951–1,722) (Figure 3A). Expression of the deletion mutants in S2 cells revealed that N950, but not C951, localized to D2 bodies, as did WT Dcr-2 (Figure 3B and Figure S3A). N950 coimmunoprecipitated with R2D2, but C951 failed to bind R2D2 (Figure 3C). Thus, the D2 body localization of Dcr-2 may coincide with Dcr-2's interaction with R2D2.

The N950 mutant was further delineated to produce three additional mutants, N694 (residues 1–694), N572 (residues 1–572), and N207 (residues 1–207) (Figure 3A). Both N694 and N572 weakly localized to D2 bodies, whereas N207 did not (Figure 3D and Figure S3B). N694 and N572 interacted with R2D2 to a lesser extent than did WT Dcr-2 (Figure 3E). N207 failed to bind R2D2 under the experimental conditions (Figure 3E). These findings are consistent with the recent finding that Dcr-2 lacking the N-terminal region (residues 1–551) does not associate with R2D2 (Hartig and Förstemann, 2011). The findings also suggest that the N-terminal region of Dcr-2 containing the HELN and HELC (RNA helicase) domains maintains its association with R2D2 and localizes to D2 bodies. Dcr-2 localization to D2 bodies indeed coincides with Dcr-2's interaction with R2D2. D2 body localization and R2D2 binding aspects of Dcr-2 WT and mutants are summarized in Figure 3A.

The dsRNA-Binding Activity and the Auxiliary Domain of R2D2 Are Required for D2 Body Formation

We next examined which part of R2D2 is required for D2 body formation. R2D2 WT and two deletion mutants, R1R2 (residues 1–166 consisting of two dsRBD domains) and Aux (residues 167–311 containing the auxiliary domain) (Figure 4A), were expressed in S2 cells, and immunofluorescence was performed. myc-tagged full-length R2D2 WT localized to D2 bodies, but neither myc-R1R2 nor myc-Aux did (Figure 4B and Figure S4). Aux was then extended toward the N-terminal end to produce another mutant, R2Aux, to cover the second dsRNA-binding domain of R2D2 (dsRBD2) (residues 82–311) (Figure 4A). This mutant R2Aux accumulated to D2 bodies, as did R2D2 WT (Figure 4B and Figure S4), suggesting that both dsRBD2 and the auxiliary domains are necessary for R2D2 to form D2 bodies.

We then constructed another mutant, R2Aux-M, in which two residues highly conserved in dsRBDs, A153 and A154, were substituted with Glu and Asp, respectively (Figure 4A) (Liu et al., 2006; also see the Experimental Procedures). This mutation abolishes the dsRNA-binding activity of R2D2 (Liu et al., 2006). R2Aux-M did not accumulate to D2 bodies (Figure 4B and Figure S4). Immunoprecipitation experiments showed that WT R2D2, R2Aux, and R2Aux-M bound Dcr-2 to a similar extent (Figure 4C), while the level of Dcr-2 associated with R1R2 was near the background level. Aux associated with Dcr-2, but not as strongly as did WT R2D2 (Figure 4C). Thus, dsRBD2 stabilizes the association between Dcr-2 and R2D2, but the dsRNA-binding activity of dsRBD2 is not necessary for maintaining their association. The dsRNA-binding activity of dsRBD2 was required for R2D2 to localize to D2 bodies (Figure 4B and Figure S4). Previous studies have shown that the dsRNA-binding activity of R2D2 is required for Dcr-2 to efficiently bind siRNA duplexes (Liu et al., 2003, 2006). Thus, D2 body localization of the Dcr-2-R2D2 heterodimer might depend on the dsRNA-binding status of the heterodimer. D2 body localization and Dcr-2 binding aspects of R2D2 WT and mutants are summarized in Figure 4A.

R2D2 Dependency of Endo-siRNA- and Exo-siRNA-Specific Sorting onto Ago2 In Vivo

In *r2d2* mutants, very few endo-siRNAs are loaded onto Ago2, with most being misdirected to Ago1 (Okamura et al., 2011). We sought to examine if this phenomenon would be recapitulated in S2 cells. R2D2 was depleted from S2 cells by RNAi, and then Flag-Ago1 and Flag-Ago2 were expressed individually. Northern blotting was performed on RNAs isolated from the Flag-Ago1 and Flag-Ago2 complexes immunoprecipitated using an anti-Flag antibody (Figure S5A). We found that esiR-sl-1, an endo-siRNA expressed in S2 cells (Kawamura et al., 2008), was loaded onto Ago2 to a similar extent to that seen in luciferase (luc) RNAi-treated cells, suggesting that R2D2 is dispensable for endo-siRNA loading onto Ago2 in S2 cells (Figure 5A). D2 bodies are not formed without R2D2 expression (Figure 2A), indicating that endo-siRNA loading onto Ago2 occurs D2 body independently in the cytosol.

Endo-siRNAs were aberrantly loaded onto Ago1 when R2D2 was lacking in S2 cells (Figure 5A). Thus, R2D2 is required for preventing endo-siRNA misdirection onto Ago1 in S2 cells. The distribution of miR-bantam, an miRNA expressed in S2 cells, between Ago1 and Ago2 was hardly affected in R2D2-lacking cells (Figure 5A); thus, Ago1 favors miRNAs even under aberrant conditions in which endo-siRNAs are also available for Ago1 to bind. The total level of esiR-sl-1 was higher (~3-fold) in R2D2-depleted S2 cells than in control cells (Figure 5A and Figure S5B). R2D2 depletion led to D2 body disruption, and Dcr-2 alone was

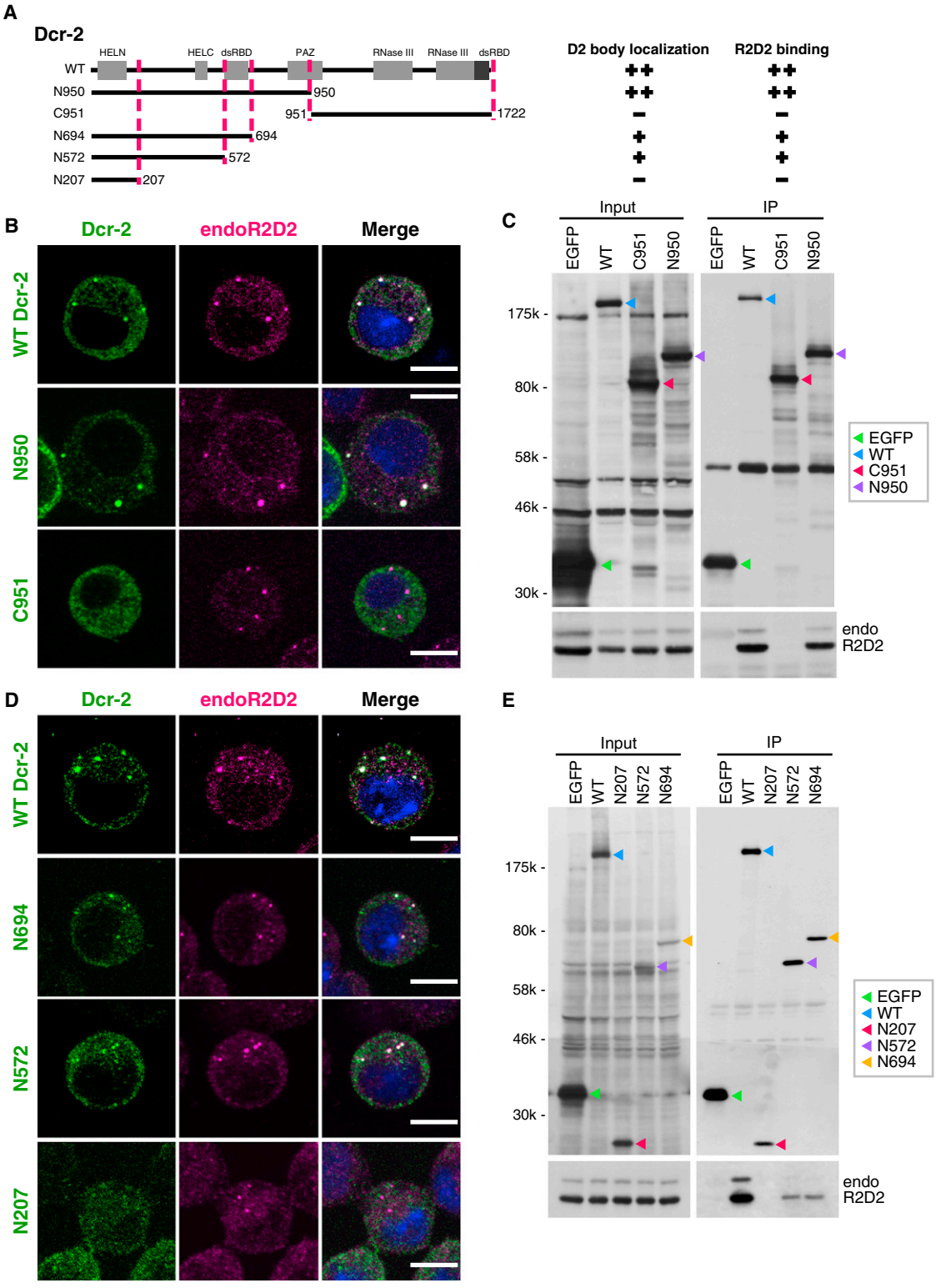

Figure 3. Dcr-2 N Terminus Interacts with R2D2 and Localizes to D2 Bodies

(A) The domain structure of Dcr-2 WT and deletion mutants. D2 body localization and R2D2 binding of Dcr-2 WT and mutants are summarized on the right.

(B) A Dcr-2 deletion mutant, N950, consisting of the N-terminal half of Dcr-2, localizes to D2 bodies, as does Dcr-2 WT. By contrast, the C-terminal half of Dcr-2, C951, fails to localize to D2 bodies. Dcr-2 WT, N950, and C951 were tagged with a 3xFlag peptide (green). Endogenous R2D2 is detected by anti-R2D2 antibody (magenta). Nuclei are stained with DAPI (blue). Scale bars, 5 μm.

(legend continued on next page)

released into the cytosol (Figure 2A). Dcr-2 floating in the cytosol might have enhanced endo-siRNA processing, resulting in a higher level of endo-siRNAs in the cells. Northern blotting with a DNA probe detecting esiR-sl-1* (the antisense strand of esiR-sl-1) failed to detect esiR-sl-1* in Ago1 and Ago2 complexes (Figure S5C), suggesting that strand selection of endo-siRNAs can still be maintained without R2D2. The factors controlling strand selection in the absence of R2D2 remain to be determined.

We set out to determine if exo-siRNAs are loaded onto Ago2 R2D2 independently. R2D2-depleted S2 cells were transfected with exo-siRNA along with a vector for expressing Flag-Ago1 or Flag-Ago2. Northern blotting was performed on total RNAs in the immunoprecipitated Flag-Ago1 and Flag-Ago2 complexes using two probes recognizing the guide and passenger strands, individually. Both strands were detected in immunoprecipitates obtained from R2D2-depleted S2 cells expressing Flag-Ago2, but not in those obtained from cells expressing Flag-Ago1, in R2D2-depleted cells, suggesting that exo-siRNAs are loaded specifically onto Ago2 R2D2 independently (Figure 5B and Figure S5D). Depletion of Dcr-2, which destabilizes both Dcr-2 and R2D2 (Figure 2B), did not affect exo-RNA loading onto Ago2 (Figure 5B and Figure S5D). Thus, both exo-siRNA sorting onto Ago2 and miRNA sorting onto Ago1 occur R2D2/Dcr-2 independently. The guide strand, but not the passenger strand, of exo-siRNA duplex was loaded onto Ago2 (Figure S5E). Thus, guide strand selection of siRNAs occurs R2D2 independently. exo-siRNA duplexes are fully complementary, while endo-siRNA duplexes show mostly incomplete complementarity (Czech et al., 2008; Ghildiyal et al., 2008; Kawamura et al., 2008; Okamura et al., 2008). This may be the cause of the difference between exo-siRNAs and endo-siRNAs in terms of their R2D2 dependency of Argonaute sorting. It has been shown that small RNA duplexes with full complementarity were loaded onto Ago2, while those with incomplete complementarity were loaded onto Ago1 in in vitro assays (Tomari et al., 2007).

The Ability of R2D2 to Localize Dcr-2 to D2 Bodies Is Required for Endo-siRNA Sorting onto Ago2

We then examined if expression of RNAi-resistant R2D2 is able to rescue the R2D2 defective phenotype in S2 cells. Endogenous R2D2 was knocked down by a specific R2D2-siRNA, and then RNAi-resistant R2D2 WT (R2D2 WT-R) was expressed (Figure S5F). As expected, R2D2 depletion caused endogenous Dcr-2 to become dispersed in the cytosol (Figure 5C and Figure S6A). Expression of R2D2 WT-R in R2D2-depleted cells restored D2 bodies (Figure 5C and Figure S6A). Northern blotting of total RNAs isolated from Flag-Ago1 and Flag-Ago2 complexes showed that R2D2 WT-R was able to restore specific endo-siRNA loading onto Ago2 (Figure 5D).

Immunofluorescence analyses showed that expression of R2Aux in R2D2-depleted cells was able to restore D2 body formation, but that expression of R2Aux-M was not (Figure 5C). We then asked if these mutants are able to rescue misloading of endo-siRNA onto Ago1 in R2D2-depleted cells. R2Aux, but not R2Aux-M, rescued the defective phenotype (Figure 5E and Figure S6B). These findings suggest that Dcr-2 localization to D2 bodies is directly linked to prevention of endo-siRNA misloading onto Ago1.

Ago1, which forms a complex with miRNAs and their target mRNAs, accumulates in P bodies, where the miRNA target is eventually degraded (Behm-Ansmant et al., 2006). By immunofluorescence, Flag-Ago1 showed a similar distribution to Dcp1, Tral, and Me31B in S2 cells with and without cycloheximide and puromycin treatments (Figure 1B, Figures S1A and S6C). Thus, Ago1 is not a component of D2 bodies. Flag-Ago2 in S2 cells was mostly localized in the cytosol (Figure S6D). However, Flag-Ago2 was also found in D2 bodies, and these signals were resistant to cycloheximide treatment (Figure S6E). Ago2 might localize to D2 bodies in S2 cells, albeit transiently.

DISCUSSION

In this study, we show that R2D2 localizes Dcr-2, presumably together with endo-siRNA duplexes, to D2 bodies to ensure endo-siRNA-specific loading onto Ago2 (and to prevent endo-siRNA misloading onto Ago1) in S2 cells (Figure 6A). Depletion of R2D2 causes D2 bodies to collapse. Under this circumstance, endo-siRNAs can still be loaded onto Ago2; however, concomitantly, Ago1 starts misloading endo-siRNAs in the cytosol (Figure 6B). This is because Ago1 has the ability to accommodate siRNA duplexes showing incomplete complementarity (Tomari et al., 2007; Czech and Hannon, 2011). In regular S2 cells, exo-siRNAs might be loaded onto Ago2 in a fashion equivalent to that for endo-siRNAs (Figure 6A). In cells lacking D2 bodies, exo-siRNAs are still loaded onto Ago2 (Figure 6B), because Ago1 avoids binding fully complementary small RNA duplexes (Tomari et al., 2007; Czech and Hannon, 2011). miRNA loading onto Ago1 does not seem to require such a regulatory system for loading, because Ago1 prefers to bind small RNA duplexes with incomplete complementarity. We propose that D2 bodies are the cellular location where endo-siRNA loading onto Ago2 occurs (Figure 6A), although we cannot exclude the possibility that some endo-siRNAs may be loaded onto Ago2 in the cytosol, outside of D2 bodies, Dcr-2-R2D2 dependently or independently. The "inside D2 bodies" theory is favorable, because localized concentration of the necessary factors might enhance the rate of the loading reaction. Upon loading of an siRNA duplex onto Ago2, the Dcr-2/R2D2 heterodimer might leave D2 bodies to associate with siRNA duplexes in the cytosol, and then go back to D2 bodies (Figure 6A). This model for intracellular,

(C) Immunoprecipitation followed by western blotting shows that Flag-Dcr-2 WT and Flag-N950, but not Flag-C951, bind R2D2. Flag-EGFP was used as a negative control.
(D) N950 was further delineated to produce the mutants N694, N572, and N207 (see A). All Dcr-2 mutants and WT Dcr-2 are Flag tagged (3xFlag) and were detected using anti-Flag antibody (green). N694 and N572 weakly localize to D2 bodies, but N207 did not. Endogenous R2D2 is shown in magenta. Nuclei are stained with DAPI (blue). Scale bars, 5 μm.
(E) Flag-N694 and Flag-N572 weakly associate with R2D2, while Flag-N207 failed to bind R2D2. Flag-EGFP was used as a negative control. See also Figure S3.

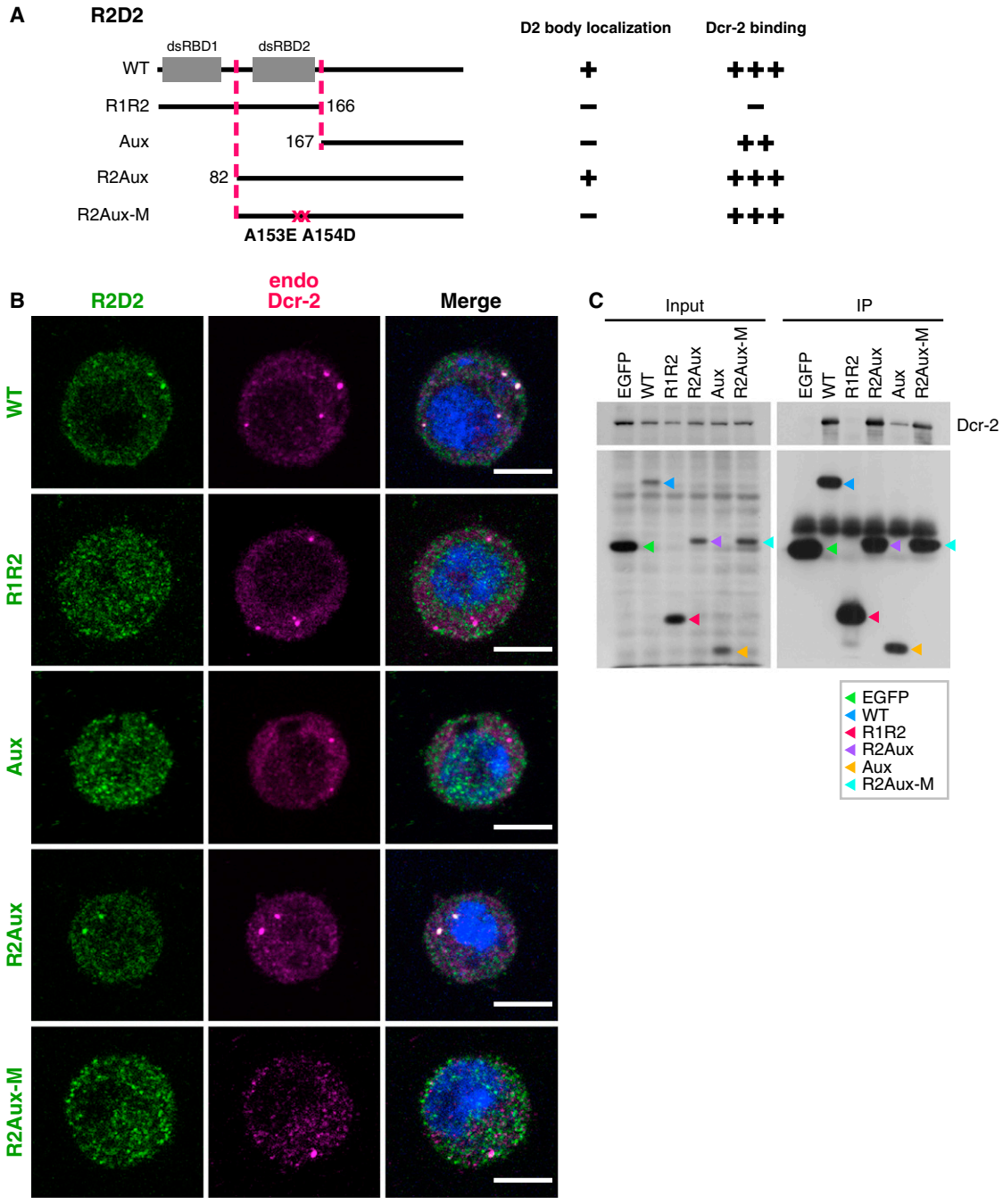

Figure 4. The dsRNA-Binding Activity and the Auxiliary Domain of R2D2 Are Required for Association with Dcr-2 and D2 Body Localization

(A) The domain structure of R2D2 WT and its deletion mutants. D2 body localization and Dcr-2 binding of R2D2 WT and mutants are summarized on the right.

(B) R2D2 WT localizes to D2 bodies, but two deletion mutants, R1R2 and Aux, failed to do so. By contrast, R2Aux containing dsRBD2 and Aux localizes to D2 bodies. To abolish the dsRNA-binding activity of R2Aux, A153 and A154 were substituted with Glu and Asp, respectively, in the context of R2Aux. This mutant R2Aux-M no longer accumulates in D2 bodies, suggesting that the dsRNA-binding activity is necessary for R2D2 to localize to D2 bodies. R2D2 WT and all mutants are myc tagged. Scale bars, 5 μm.

(C) Immunoprecipitation followed by western blotting shows that myc-R2D2 WT, myc-R2Aux, and myc-R2Aux-M, but not myc-R1R2, bind Dcr-2 to a similar extent. myc-Aux binds Dcr-2, but weakly compared with myc-R2D2 WT. myc-EGFP was used as a negative control. See also Figure S4.

dynamic translocation of the Dcr-2/R2D2 heterodimer is consistent with the observations that heterodimers lacking dsRNA-binding activity do not localize to D2 bodies (Figure 4B) and that only a minor portion of Dcr-2 and R2D2 is localized to D2 bodies (Figure S2G). It remains unclear how D2 body formation is triggered in the cells. Identification of D2 body components

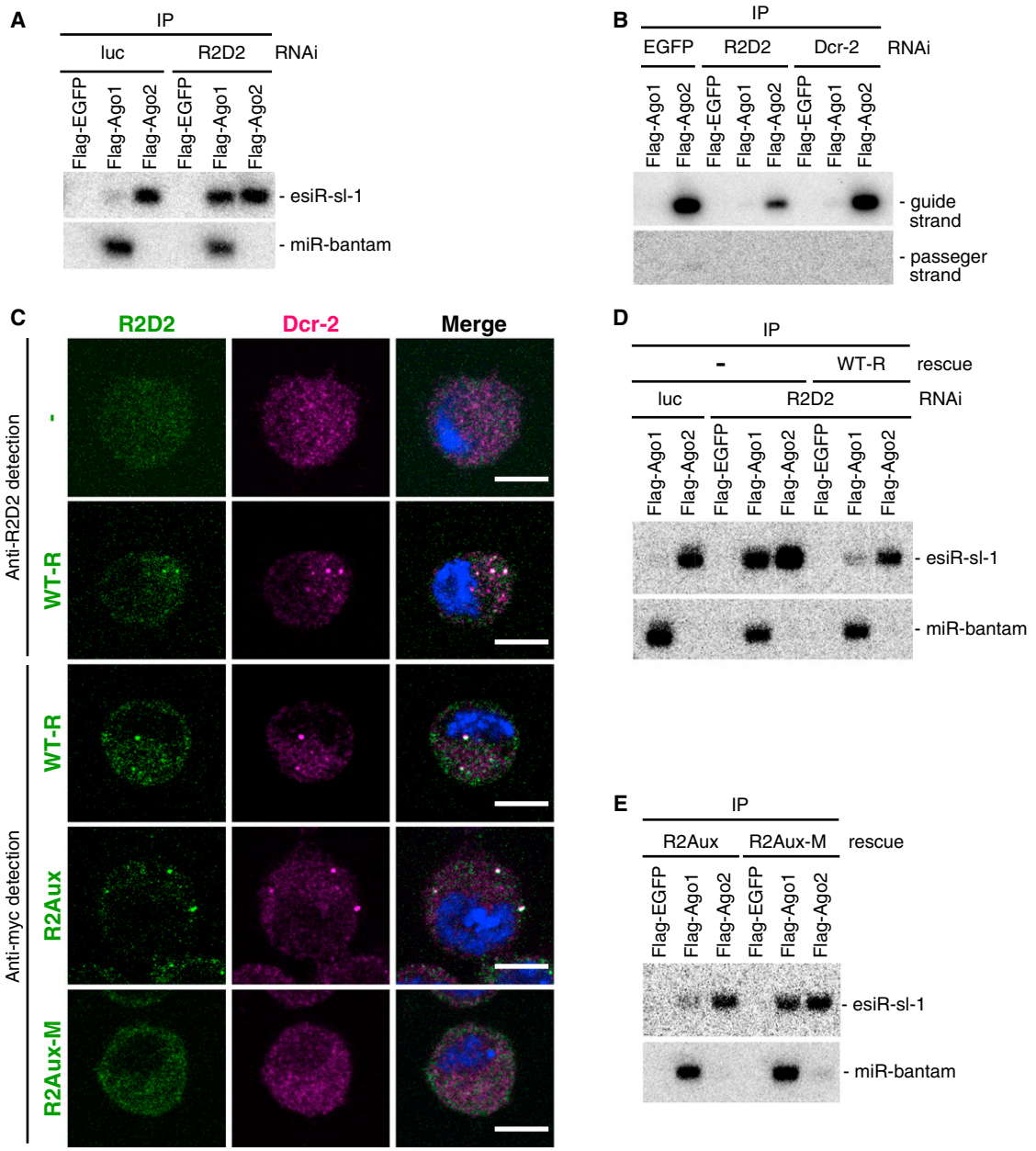

Figure 5. R2D2 Ensures Endo-siRNA Sorting onto Ago2 by Sequestering Dcr-2 to D2 Bodies

(A) Flag-Ago1 and Flag-Ago2 were expressed after R2D2 was deleted by RNAi. The endo-siRNA esiR-sl-1 is still loaded onto Ago2 in the absence of R2D2, demonstrating that R2D2 is not necessary for endo-siRNA loading onto Ago2. Under the same conditions, Ago1 also associates with esiR-sl-1. endo-siRNA misdirection onto Ago1 (Okamura et al., 2011) was also induced in S2 cells. miR-bantam was not misloaded onto Ago2.

(B) exo-siRNA was specifically loaded onto Ago2 in the absence of R2D2 and the Dcr-2/R2D2 heterodimer. The amount of proteins immunoprecipitated is shown in Figure S5D.

(C) The expression of an R2D2-siRNA-resistant form of R2D2 WT, WT-R, and R2Aux restored D2 body formation in R2D2-depleted cells, but R2Aux-M failed to do the same. R2D2 WT-R, R2Aux, and R2Aux-M were myc tagged and detected by anti-R2D2 and/or anti-myc antibodies, as indicated (green). Endogenous Dcr-2 was detected using anti-Dcr-2 antibody (magenta). Nuclei are shown in blue by DAPI staining. Scale bars, 5 μm.

(D) Expression of R2D2 WT-R rescues the R2D2-defective phenotype, endo-siRNA misloading onto Ago1, in R2D2-depleted cells.

(E) Expression of R2Aux, but not of R1Aux-M, rescues the R2D2-defective phenotype, endo-siRNA misloading onto Ago1, in R2D2-depleted cells. See also Figures S5 and S6.

other than Dcr-2 and R2D2 may help to understand the underlying mechanism, which is currently under investigation in our laboratory.

Depletion of R2D2 from S2 cells caused disappearance of D2 bodies, but in this circumstance, endo-siRNAs still associated with both Ago1 and Ago2, suggesting that endo-siRNA loading

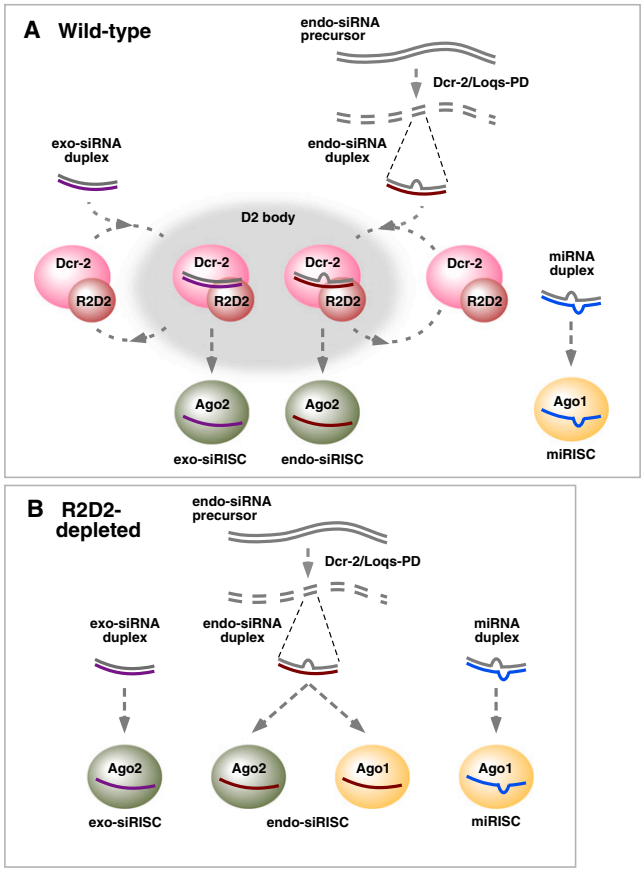

Figure 6. A Model for R2D2's Function in Controlling Endo-siRNA Sorting in *Drosophila* S2 Cells

(A) In *Drosophila* S2 cells (wild-type), R2D2 localizes Dcr-2, and presumably endo-siRNA duplexes, into D2 bodies to ensure endo-siRNA loading onto Ago2. This reaction yields the endo-siRISC. Ago1 does not localize to D2 bodies; thus, endo-siRNA misdirection onto Ago1 is avoided. exo-siRNAs might also be loaded onto Ago2 in a fashion equivalent to that for endo-siRNAs. This reaction yields the exo-siRISC. miRNAs are loaded onto Ago1 in a manner independent of D2 bodies, which yields the miRISC. Upon loading of siRNA duplex onto Ago2, the Dcr-2/R2D2 heterodimer leaves D2 bodies to associate with siRNA duplexes in the cytosol and then goes back to D2 bodies. (B) In R2D2-depleted *Drosophila* cells (R2D2-depleted), D2 bodies collapse and Dcr2 is orphaned in the cytosol. In this circumstance, endo-siRNAs are loaded onto not only Ago2 but also Ago1. This loading might occur without the help of Dcr-2, because R2D2, or its dsRNA-binding activity, is required for Dcr-2 to efficiently bind siRNA duplexes and load them onto Ago2 (Liu et al., 2003, 2006). Strand selection is still maintained, although the underlying mechanism remains unknown. exo-siRNAs are specifically loaded onto Ago2, while miRNAs are still specifically loaded onto Ago1.

onto Argonaute proteins does not absolutely require R2D2. It has been reported that R2D2 plays a crucial role in the asymmetrical selection of guide exo-siRNAs from exo-siRNA duplexes (Tomari et al., 2007). However, in our study, esiR-sl-1* was not detected in Ago1 and Ago2 complexes, unlike esiR-sl-1, which was detected in R2D2-depleted cells. We also found that guide exo-siRNA was also selectively loaded onto Ago2 in Dcr-2- and R2D2-depleted cells. Thus, R2D2 is not absolutely required for siRNA strand selection in vivo. One possibility is that Argonaute proteins alone can implement endo-siRNA and exo-siRNA strand selection. We are currently exploring this possibility in our laboratory.

The level of miRNAs associated with Ago1 was hardly changed by R2D2 depletion in S2 cells (Figure 5A). A recent study showed that miRNAs are loaded onto Ago1 as efficiently in *r2d2* mutant flies as they are in WT flies (Okamura et al., 2011). One explanation for these observations is that the expression level of Ago1 is so high that endo-siRNA misloading onto Ago1 does not disturb Ago1-miRNA binding and Ago1 functions. Another explanation is that there is an inherent mechanism in cells that forces Ago1 to favor miRNAs even in circumstances in which endo-siRNAs and miRNAs are equally available for Ago1 to bind.

If the latter possibility is correct, what would be the biological relevance for *Drosophila*? There are potentially two scenarios: the "endo-siRNA function protection" scenario and the "miRNA function protection" scenario. It has been shown that Ago1's Slicer activity (endonuclease activity to cleave its target transcripts) is much weaker than that of Ago2 (Förstemann et al., 2007). This means that endo-siRNAs misdirected to Ago1 would not be able to exhibit sufficiently the intrinsic activity of endo-siRNAs to silence transposons by cleaving the transcripts. Many species, including flies, nematodes, and plants, are equipped with an siRNA-mediated gene silencing pathway (or RNAi) as an innate immune system to protect themselves from life-threatening, invasive viruses and/or transposons randomly inserting copies of themselves into the host genome (Ding and Voinnet, 2007). To control this system, animals and plants have developed systems to fully maintain siRNA functions (the "endo-siRNA function protection" scenario).

Endo-siRNAs act as an innate immune system, while miRNAs function to maintain cellular gene networks by regulating the expression of many of the genes involved in them. In mammals, the two pathways share some proteins as common factors: for instance, Argonaute proteins. However, *Drosophila* basically maintains these pathways independently. This notion is strongly supported by the observations that *Drosophila* distinguishably uses Dcr-1 and Ago1, and Dcr-2 and Ago2, which are dedicated to the miRNA and siRNA pathways, respectively, although it should be noted that some crosstalk between these pathways has been previously reported (Ghildiyal and Zamore, 2009; Ghildiyal et al., 2010). Keeping the independency of these pathways is crucial for *Drosophila*, because, unlike mammals, flies do not have other immune systems for protecting themselves from infectious viruses. Thus, *Drosophila* has had to develop mechanisms to maintain the independency of the miRNA and siRNA pathways. One such mechanism is the one preventing endo-siRNA misloading onto Ago1 (the "miRNA function protection" scenario).

EXPERIMENTAL PROCEDURES

Immunofluorescence

Immunofluorescence was performed after fixing S2 cells with 2% formaldehyde for 15 min at room temperature. Cells were permeabilized with 0.1% Triton X-100 and then, after washing, stained with anti-Dcr-2 (Miyoshi et al., 2009), anti-R2D2 (this study), anti-Dcp1 (Miyoshi et al., 2009), anti-dFMR1 (Okamura et al., 2004), and anti-dGM130 (Yano et al., 2005) antibodies. To

detect Flag-Dcr-2 WT and mutants, cells were stained with anti-Flag (M2) antibody (Sigma-Aldrich). To detect myc-tagged R2D2 WT and mutants, anti-myc (9E10) antibody (Sigma-Aldrich) was used. Alexa Fluor 488/555 goat anti-mouse IgG1/IgG2a/IgG2b (Invitrogen) and Alexa Flour 488 goat anti-rabbit IgG (H^+L) were used as secondary antibodies. Monoclonal antibodies against R2D2 were produced using full-length R2D2 tagged with GST as an antigen, as described previously (Miyoshi et al., 2009). S2 cells were treated with cycloheximide (10 μg/ml) and puromycin (100 μg/ml) for 1 hr (Eulalio et al., 2007b) before immunofluorescence. Arsenite treatment was performed at final concentration of 500 μM for 2 hr (Farny et al., 2009).

Plasmid Construction

Expression vectors of Flag-Dcr-2 WT and deletion mutants were generated by inserting the corresponding coding regions into the pRH3xflag vector (Saito et al., 2005). DNA oligos used for Dcr-2 mutant construction are shown in Table S1. Expression vectors of myc-R2D2 WT and deletion mutants were generated by inserting the corresponding coding region into the pAcM vector (Saito et al., 2009). DNA oligos used for R2D2 mutant construction are shown in Table S1. Liu et al. (2006) described that A153 and A154 were mutated to two lysines. However, we found by sequencing the original mutant construct from that group that they were actually mutated to Glu and Asp, respectively, which was confirmed by Q. Liu (Liu et al., 2006). To yield RNAi-resistant R2D2 WT, two primers, R2D2-R-F and R2D2-R-R, were used (Table S1) for PCR. PCR was carried out using KOD plus DNA polymerase (Toyobo).

RNAi

RNAi was performed in S2 cells as described previously (Saito et al., 2005). dsRNA used for R2D2 depletion corresponded to nucleotides 1–820 of the R2D2 coding sequence. dsRNAs for Dcr-2 and EGFP were described previously (Saito et al., 2005). S2 cells (3×10^6 cells) were suspended in 100 μl of Solution V of the Cell Line Nucleofector Kit V (Amaxa Biosystems) with 200 pmol of siRNA duplex. Transfection was conducted in electroporation cuvettes using Nucleofector (Amaxa Biosystems). After transfection, cells were transferred to fresh medium and incubated at 26°C for 3 days for further experiments. The siRNAs used for RNAi are summarized in Table S1. Luc siRNA (Saito et al., 2009) was used as a control. The sequences of siRNAs used in the experiments are shown in Table S1.

Northern Blot Analysis

Northern blot analysis was carried out essentially as described previously using 1-ethyl-3-(3-dimethylaminopropyl) carbodiimide (EDC) (Saito et al., 2010). The sequences of the DNA oligos for esiR-sl-1 and miR-bantam are indicated in Kawamura et al. (2008). The DNA oligos used to detect siRNA guide and passenger strands are 5′-AAATAGATAATAGTCATTGGC-3′ (guide) and 5′-AAGCCAATGACTATTATCTAT-3′ (passenger) (Figure 5B).

Immunoprecipitation and Western Blotting

The Flag-Dcr-2 WT and mutant complexes were immunopurified from S2 cells using anti-Flag M2 agarose beads (Sigma-Aldrich). The myc-R2D2 WT and mutant complexes were immunopurified from S2 cells using anti-myc antibody (9E10) bound to Dynabeads protein G (Invitrogen). After immunoprecipitation, the beads were washed extensively with binding buffer containing 30 mM HEPES (pH 7.4), 150 mM potassium acetate, 5 mM magnesium acetate, 5 mM DTT, 0.1% Nonidet P-40, 2 μg/mL pepstatin, 2 μg/mL leupeptin, and 0.5% aprotinin. Western blotting was performed as described previously (Miyoshi et al., 2005). Anti-tubulin antibody was obtained from the Developmental Studies Hybridoma Bank and used at a 1:1,000 dilution. To purify Flag-Ago1 and Flag-Ago2, immunoprecipitation was performed using anti-Flag M2 agarose beads. After immunoprecipitation, the beads were washed extensively with binding buffer containing 500 mM sodium chloride and then with binding buffer.

SUPPLEMENTAL INFORMATION

Supplemental Information includes six figures, one table, Supplemental Experimental Procedures, and Supplemental References and can be found with this article at http://dx.doi.org/10.1016/j.molcel.2012.12.024.

ACKNOWLEDGMENTS

We thank Q. Liu for the R2D2 mutant plasmid; S. Goto for the dGM130 antibody; and T.N. Okada, A. Takeuchi, and T. Sunohara for technical assistance and reagents. We are thankful to M. Isogai and M. Shimura (PerkinElmer Japan) for their assistance with fluorescence quantification. We also thank the other members of the Siomi laboratories for discussions and comments on the manuscript. This work was supported by MEXT grants (to H.S., K.M., and M.C.S.) and by grants from the Uehara Memorial Foundation (to K.M.). M.C.S. is supported by CREST from JST.

Received: July 16, 2012
Revised: November 16, 2012
Accepted: December 26, 2012
Published: January 31, 2013

REFERENCES

Ameres, S.L., Hung, J.H., Xu, J., Weng, Z., and Zamore, P.D. (2011). Target RNA-directed tailing and trimming purifies the sorting of endo-siRNAs between the two *Drosophila* Argonaute proteins. RNA *17*, 54–63.

Barbee, S.A., Estes, P.S., Cziko, A.-M., Hillebrand, J., Luedeman, R.A., Coller, J.M., Johnson, N., Howlett, I.C., Geng, C., Ueda, R., et al. (2006). Staufen- and FMRP-containing neuronal RNPs are structurally and functionally related to somatic P bodies. Neuron *52*, 997–1009.

Behm-Ansmant, I., Rehwinkel, J., Doerks, T., Stark, A., Bork, P., and Izaurralde, E. (2006). mRNA degradation by miRNAs and GW182 requires both CCR4:NOT deadenylase and DCP1:DCP2 decapping complexes. Genes Dev. *20*, 1885–1898.

Bernstein, E., Denli, A.M., and Hannon, G.J. (2001). The rest is silence. RNA *7*, 1509–1521.

Czech, B., and Hannon, G.J. (2011). Small RNA sorting: matchmaking for Argonautes. Nat. Rev. Genet. *12*, 19–31.

Czech, B., Malone, C.D., Zhou, R., Stark, A., Schlingeheyde, C., Dus, M., Perrimon, N., Kellis, M., Wohlschlegel, J.A., Sachidanandam, R., et al. (2008). An endogenous small interfering RNA pathway in *Drosophila*. Nature *453*, 798–802.

Denli, A.M., Tops, B.B., Plasterk, R.H., Ketting, R.F., and Hannon, G.J. (2004). Processing of primary microRNAs by the Microprocessor complex. Nature *432*, 231–235.

Ding, S.W., and Voinnet, O. (2007). Antiviral immunity directed by small RNAs. Cell *130*, 413–426.

Eulalio, A., Behm-Ansmant, I., and Izaurralde, E. (2007a). P bodies: at the crossroads of post-transcriptional pathways. Nat. Rev. Mol. Cell Biol. *8*, 9–22.

Eulalio, A., Behm-Ansmant, I., Schweizer, D., and Izaurralde, E. (2007b). P-body formation is a consequence, not the cause, of RNA-mediated gene silencing. Mol. Cell. Biol. *27*, 3970–3981.

Farny, N.G., Kedersha, N.L., and Silver, P.A. (2009). Metazoan stress granule assembly is mediated by P-eIF2alpha-dependent and -independent mechanisms. RNA *15*, 1814–1821.

Förstemann, K., Tomari, Y., Du, T., Vagin, V.V., Denli, A.M., Bratu, D.P., Klattenhoff, C., Theurkauf, W.E., and Zamore, P.D. (2005). Normal microRNA maturation and germ-line stem cell maintenance requires Loquacious, a double-stranded RNA-binding domain protein. PLoS Biol. *3*, e236.

Förstemann, K., Horwich, M.D., Wee, L., Tomari, Y., and Zamore, P.D. (2007). *Drosophila* microRNAs are sorted into functionally distinct argonaute complexes after production by dicer-1. Cell *130*, 287–297.

Ghildiyal, M., and Zamore, P.D. (2009). Small silencing RNAs: an expanding universe. Nat. Rev. Genet. *10*, 94–108.

Ghildiyal, M., Seitz, H., Horwich, M.D., Li, C., Du, T., Lee, S., Xu, J., Kittler, E.L., Zapp, M.L., Weng, Z., and Zamore, P.D. (2008). Endogenous siRNAs derived from transposons and mRNAs in *Drosophila* somatic cells. Science *320*, 1077–1081.

Ghildiyal, M., Xu, J., Seitz, H., Weng, Z., and Zamore, P.D. (2010). Sorting of Drosophila small silencing RNAs partitions microRNA* strands into the RNA interference pathway. RNA *16*, 43–56.

Gregory, R.I., Yan, K.P., Amuthan, G., Chendrimada, T., Doratotaj, B., Cooch, N., and Shiekhattar, R. (2004). The Microprocessor complex mediates the genesis of microRNAs. Nature *432*, 235–240.

Hartig, J.V., and Förstemann, K. (2011). Loqs-PD and R2D2 define independent pathways for RISC generation in Drosophila. Nucleic Acids Res. *39*, 3836–3851.

Hartig, J.V., Esslinger, S., Böttcher, R., Saito, K., and Förstemann, K. (2009). Endo-siRNAs depend on a new isoform of loquacious and target artificially introduced, high-copy sequences. EMBO J. *28*, 2932–2944.

Jiang, F., Ye, X., Liu, X., Fincher, L., McKearin, D., and Liu, Q. (2005). Dicer-1 and R3D1-L catalyze microRNA maturation in *Drosophila*. Genes Dev. *19*, 1674–1679.

Kawamura, Y., Saito, K., Kin, T., Ono, Y., Asai, K., Sunohara, T., Okada, T.N., Siomi, M.C., and Siomi, H. (2008). *Drosophila* endogenous small RNAs bind to Argonaute 2 in somatic cells. Nature *453*, 793–797.

Kedersha, N., Stoecklin, G., Ayodele, M., Yacono, P., Lykke-Andersen, J., Fritzler, M.J., Scheuner, D., Kaufman, R.J., Golan, D.E., and Anderson, P. (2005). Stress granules and processing bodies are dynamically linked sites of mRNP remodeling. J. Cell Biol. *169*, 871–884.

Khvorova, A., Reynolds, A., and Jayasena, S.D. (2003). Functional siRNAs and miRNAs exhibit strand bias. Cell *115*, 209–216.

Kim, V.N., Han, J., and Siomi, M.C. (2009). Biogenesis of small RNAs in animals. Nat. Rev. Mol. Cell Biol. *10*, 126–139.

Kondylis, V., Goulding, S.E., Dunne, J.C., and Rabouille, C. (2001). Biogenesis of Golgi stacks in imaginal discs of *Drosophila melanogaster*. Mol. Biol. Cell *12*, 2308–2327.

Lee, Y., Ahn, C., Han, J., Choi, H., Kim, J., Yim, J., Lee, J., Provost, P., Rådmark, O., Kim, S., and Kim, V.N. (2003). The nuclear RNase III Drosha initiates microRNA processing. Nature *425*, 415–419.

Lee, Y.S., Nakahara, K., Pham, J.W., Kim, K., He, Z., Sontheimer, E.J., and Carthew, R.W. (2004). Distinct roles for *Drosophila* Dicer-1 and Dicer-2 in the siRNA/miRNA silencing pathways. Cell *117*, 69–81.

Liu, Q., Rand, T.A., Kalidas, S., Du, F., Kim, H.E., Smith, D.P., and Wang, X. (2003). R2D2, a bridge between the initiation and effector steps of the *Drosophila* RNAi pathway. Science *301*, 1921–1925.

Liu, X., Jiang, F., Kalidas, S., Smith, D., and Liu, Q. (2006). Dicer-2 and R2D2 coordinately bind siRNA to promote assembly of the siRISC complexes. RNA *12*, 1514–1520.

Marques, J.T., Kim, K., Wu, P.H., Alleyne, T.M., Jafari, N., and Carthew, R.W. (2010). Loqs and R2D2 act sequentially in the siRNA pathway in *Drosophila*. Nat. Struct. Mol. Biol. *17*, 24–30.

Miyoshi, K., Tsukumo, H., Nagami, T., Siomi, H., and Siomi, M.C. (2005). Slicer function of *Drosophila* Argonautes and its involvement in RISC formation. Genes Dev. *19*, 2837–2848.

Miyoshi, K., Okada, T.N., Siomi, H., and Siomi, M.C. (2009). Characterization of the miRNA-RISC loading complex and miRNA-RISC formed in the *Drosophila* miRNA pathway. RNA *15*, 1282–1291.

Miyoshi, K., Miyoshi, T., Hartig, J.V., Siomi, H., and Siomi, M.C. (2010). Molecular mechanisms that funnel RNA precursors into endogenous small-interfering RNA and microRNA biogenesis pathways in *Drosophila*. RNA *16*, 506–515.

Okamura, K., Ishizuka, A., Siomi, H., and Siomi, M.C. (2004). Distinct roles for Argonaute proteins in small RNA-directed RNA cleavage pathways. Genes Dev. *18*, 1655–1666.

Okamura, K., Chung, W.J., Ruby, J.G., Guo, H., Bartel, D.P., and Lai, E.C. (2008). The *Drosophila* hairpin RNA pathway generates endogenous short interfering RNAs. Nature *453*, 803–806.

Okamura, K., Robine, N., Liu, Y., Liu, Q., and Lai, E.C. (2011). R2D2 organizes small regulatory RNA pathways in *Drosophila*. Mol. Cell. Biol. *31*, 884–896.

Pham, J.W., Pellino, J.L., Lee, Y.S., Carthew, R.W., and Sontheimer, E.J. (2004). A Dicer-2-dependent 80s complex cleaves targeted mRNAs during RNAi in Drosophila. Cell *117*, 83–94.

Saito, K., Ishizuka, A., Siomi, H., and Siomi, M.C. (2005). Processing of pre-microRNAs by the Dicer-1-Loquacious complex in *Drosophila* cells. PLoS Biol. *3*, e235. http://dx.doi.org/10.1371/journal.pbio.0030235.

Saito, K., Inagaki, S., Mituyama, T., Kawamura, Y., Ono, Y., Sakota, E., Kotani, H., Asai, K., Siomi, H., and Siomi, M.C. (2009). A regulatory circuit for *piwi* by the large Maf gene *traffic jam* in *Drosophila*. Nature *461*, 1296–1299.

Saito, K., Ishizu, H., Komai, M., Kotani, H., Kawamura, Y., Nishida, K.M., Siomi, H., and Siomi, M.C. (2010). Roles for the Yb body components Armitage and Yb in primary piRNA biogenesis in *Drosophila*. Genes Dev. *24*, 2493–2498.

Schwarz, D.S., Hutvágner, G., Du, T., Xu, Z., Aronin, N., and Zamore, P.D. (2003). Asymmetry in the assembly of the RNAi enzyme complex. Cell *115*, 199–208.

Siomi, H., and Siomi, M.C. (2009). On the road to reading the RNA-interference code. Nature *457*, 396–404.

Siomi, M.C., Sato, K., Pezic, D., and Aravin, A.A. (2011). PIWI-interacting small RNAs: the vanguard of genome defence. Nat. Rev. Mol. Cell Biol. *12*, 246–258.

Tomari, Y., Matranga, C., Haley, B., Martinez, N., and Zamore, P.D. (2004). A protein sensor for siRNA asymmetry. Science *306*, 1377–1380.

Tomari, Y., Du, T., and Zamore, P.D. (2007). Sorting of Drosophila small silencing RNAs. Cell *130*, 299–308.

Vagin, V.V., Sigova, A., Li, C., Seitz, H., Gvozdev, V., and Zamore, P.D. (2006). A distinct small RNA pathway silences selfish genetic elements in the germline. Science *313*, 320–324.

Wan, L., Dockendorff, T.C., Jongens, T.A., and Dreyfuss, G. (2000). Characterization of dFMR1, a Drosophila melanogaster homolog of the fragile X mental retardation protein. Mol. Cell. Biol. *20*, 8536–8547.

Yano, H., Yamamoto-Hino, M., Abe, M., Kuwahara, R., Haraguchi, S., Kusaka, I., Awano, W., Kinoshita-Toyoda, A., Toyoda, H., and Goto, S. (2005). Distinct functional units of the Golgi complex in *Drosophila* cells. Proc. Natl. Acad. Sci. USA *102*, 13467–13472.

Zhou, R., Czech, B., Brennecke, J., Sachidanandam, R., Wohlschlegel, J.A., Perrimon, N., and Hannon, G.J. (2009). Processing of *Drosophila* endo-siRNAs depends on a specific Loquacious isoform. RNA *15*, 1886–1895.